






Using rotation number to detect sticky orbits in Hamiltonian systems

Cite as: Chaos 29, 043125 (2019); <https://doi.org/10.1063/1.5078533>

Submitted: 25 October 2018 . Accepted: 03 April 2019 . Published Online: 24 April 2019

Moises S. Santos , Michele Mugnaine, José D. Szezech , Antonio M. Batista , Iberê L. Caldas , and Ricardo L. Viana 



View Online



Export Citation



CrossMark

AIP Author Services
English Language Editing



Using rotation number to detect sticky orbits in Hamiltonian systems

Cite as: Chaos 29, 043125 (2019); doi: 10.1063/1.5078533

Submitted: 25 October 2018 · Accepted: 3 April 2019 ·

Published Online: 24 April 2019



View Online



Export Citation



CrossMark

Moises S. Santos,^{1,2} Michele Mugnaine,^{1,2} José D. Szezech, Jr.,³ Antonio M. Batista,³ Iberê L. Caldas,⁴ and Ricardo L. Viana¹

AFFILIATIONS

¹Departamento de Física, Universidade Federal do Paraná, Curitiba 80060-000, PR, Brazil

²Pós-Graduação em Ciências, Universidade Estadual de Ponta Grossa, Ponta Grossa 84030-900, PR, Brazil

³Departamento de Matemática e Estatística, Universidade Estadual de Ponta Grossa, Ponta Grossa 84030-900, PR, Brazil

⁴Instituto de Física, Universidade de São Paulo, São Paulo 05508-900, SP, Brazil

ABSTRACT

In Hamiltonian systems, depending on the control parameter, orbits can stay for very long times around islands, the so-called stickiness effect caused by a temporary trapping mechanism. Different methods have been used to identify sticky orbits, such as recurrence analysis, recurrence time statistics, and finite-time Lyapunov exponent. However, these methods require a large number of map iterations and to know the island positions in the phase space. Here, we show how to use the small divergence of bursts in the rotation number calculation as a tool to identify stickiness without knowing the island positions. This new procedure is applied to the standard map, a map that has been used to describe the dynamic behavior of several nonlinear systems. Moreover, our procedure uses a small number of map iterations and is proper to identify the presence of stickiness phenomenon for different values of the control parameter.

Published under license by AIP Publishing. <https://doi.org/10.1063/1.5078533>

Many dynamical systems can be described by Hamiltonians, such as charged particles in an electromagnetic field, planetary system, and mechanical oscillators. To investigate dynamical properties of these Hamiltonian systems, area-preserving chaotic maps, as the standard map (SM), have been introduced. One reported characteristic property is the stickiness effect that maintains orbits for long times around islands in the phase space. In this work, we propose that the rotation number (RN) can be used as a tool to identify the stickiness phenomenon.

I. INTRODUCTION

Area-preserving maps have been introduced to model the dynamic behavior of Hamiltonian systems, as in condensed matter physics,¹ neuronal networks,² optical systems,³ biomolecular networks,⁴ and plasmas magnetically confined in tokamak.⁵ One of the most studied area-preserving maps is the standard map.⁶ It has been used to describe comet dynamics⁷ and cyclotron particle accelerator.⁸

The standard map (SM) has contributed to the knowledge of chaos in Hamiltonian systems. It is a two-dimensional map that was introduced by Taylor and independently used by Chirikov to

model the motion of charged particles in a magnetic field.⁶ This map can exhibit the coexistence of regular and chaotic dynamics, with quasiperiodic islands within the chaotic sea. Traps can emerge from this coexistence in the phase space forcing chaotic trajectories to remain in regular behavior near islands during long time intervals, the so-called stickiness.⁹

The stickiness phenomenon was first reported by Contopoulos in 1971.¹⁰ He observed the phenomenon around two islands of stability surrounded by a chaotic sea. In 1983, Karney called this phenomenon of stickiness.¹¹ After Contopoulos, many researchers studied various characteristics of stickiness. Efthymiopoulos *et al.*¹² verified that the sticky regions are limited by cantori. They found that the relation between the sticky region and asymptotic curves forms. Contopoulos and Harsoula distinguished stickiness around island of stability and in chaos.¹³ Moreover, the presence of stickiness of trajectories affects the transport of particles in the phase space.⁵

Different methods have been proposed to identify sticky orbits, such as recurrence analysis,¹⁴ recurrence time statistics,¹⁵ and finite-time Lyapunov exponent (FTLE).¹⁶ These methods require a large number of iterations of the map, as well as it is necessary to know the position of the islands in the phase space. Szezech *et al.*¹⁷ proposed the finite-time rotation number (FTRN) as a fast indicator for chaotic dynamical structures. They showed that this indicator is faster and

simpler than the finite-time Lyapunov exponent. The FTRN was considered as a diagnostic tool to identify transport barriers that separate different stickiness regions in the standard nontwist map.¹⁸

In this work, we propose the rotation number (RN) as an indicator for stickiness. We show that the RN has some advantages when compared with other methods. Two important advantages are that there is no need for prior knowledge of the island positions in the phase space and the duration of the capture time intervals in order to identify the presence of stickiness. The chaotic trajectories spend a long time to return to the sticky regions, and as a consequence, in the other methods, a large number of iterations is required. Therefore, the RN becomes a faster method to verify the presence of sticky orbits.

This paper is organized as follows: In Sec. II, we introduce the standard map and the stickiness phenomenon. In Sec. III, we propose the rotation number to identify sticky orbits. In Sec. IV, we draw our conclusions.

II. STICKY ORBITS

Over the past decades, the properties of chaotic maps have been studied in great detail.¹⁹ One map that describes a variety of conservative systems is the standard map (SM), also known as the Chirikov–Taylor map.^{6,20} It is given by²¹

$$\begin{aligned} p_{n+1} &= p_n - K \sin(x_n), \\ x_{n+1} &= x_n + p_{n+1} \pmod{2\pi}, \end{aligned} \tag{1}$$

where K is the nonlinearity parameter, the variables $(x, p) \in \{[-\pi, \pi) \times [-\pi, \pi)\}$ are phase space coordinates, and $n = 0, 1, 2, \dots, N$ denote the discrete time. Equations (1) model a nonlinear oscillator under the influence of an external force,²² where p and x represent the variables moment (action) and coordinate (angle), respectively. Figures 1(a) and 1(b) show the phase space of SM for $K = 1.5$ and $K = 6.908745$, respectively. The stickiness visualization is better for $K = 6.908745$. In Fig. 1, we see that islands immerse in the chaotic sea. The chaotic orbits spend a finite time (black region) outside the islands of stability.¹⁶

Around the islands the stickiness phenomenon can appear, namely, trajectories can be imprisoned near the islands for very long times. Figures 2(a)–2(c) display magnifications around the islands for $K = 6.908745$, where some dark regions become more evident due

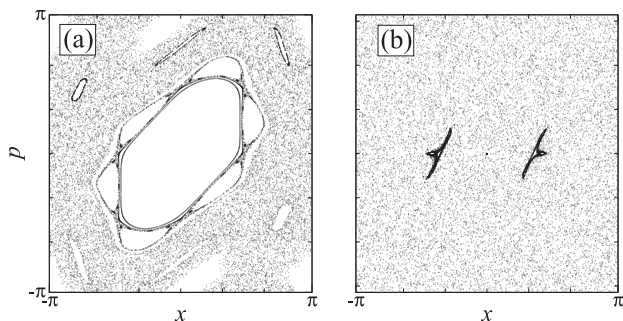


FIG. 1. Phase space of the SM for (a) $K = 1.5$ and (b) $K = 6.908745$.

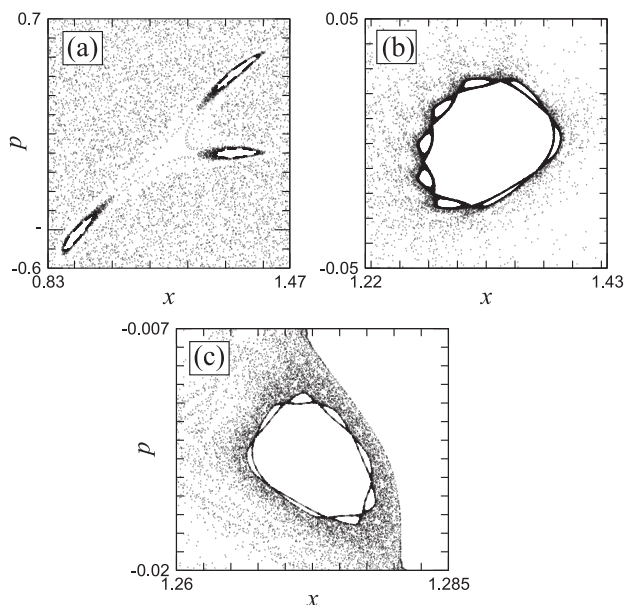


FIG. 2. Stickiness region magnifications of the phase space for $K = 6.908745$.

to the stickiness. In this way, the magnifications facilitate the visual perception of the stickiness regions due to the high density of points close to the islands. The stickiness phenomena occur due to non-hyperbolic structures.²³ A chaotic trajectory spends a long time in the vicinity of the island after crossing the barrier of a nonhyperbolic region.²⁴

As a consequence of the stickiness, a trajectory can spend a long finite time in a phase space domain. This domain is known as dynamical trap.²⁵ One of the ways to calculate the trapping time due to the

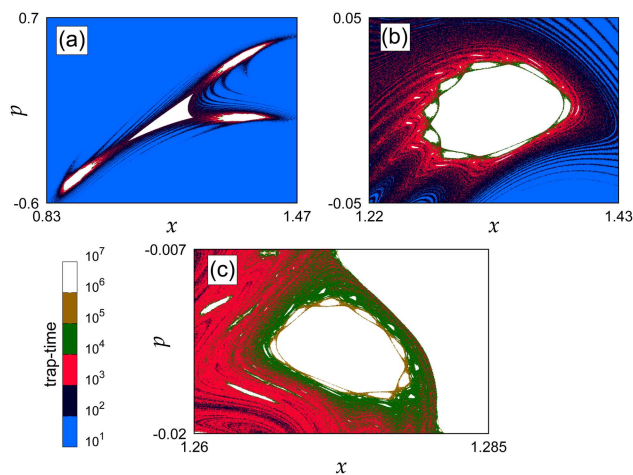


FIG. 3. Trapping time for the standard map with $K = 6.908745$ by means of the “box method,” where the color bar is in the logarithmic scale.

stickiness region is to consider a box around the position of an island and monitor the time the trajectory stays inside this box. We calculate the trapping time around the island shown in Fig. 2(a). To do that, we divide the phase space into a grid of 800×800 points and compute the trajectories for each point by means of Eq. (1). We defined the trapping time as the value of n that the trajectory stays inside the space region $-0.6 \leq p \leq 0.7$ and $0.83 \leq x \leq 1.47$ (box around the island).

Figure 3(a) exhibits the trapping time for each point in the grid for $N = 10^7$ (maximum time simulation). The not-trapped chaotic orbits remain for short times in the box (blue color), while the regular orbits (islands) remain for all time inside the box (white color). The intermediate values of time correspond to dynamical traps. In Figs. 3(a) and 3(b), the magnifications reveal the stickiness structures in the phase space. The fine structures are responsible for the trapping times.¹⁵

III. ROTATION NUMBER

In this work, we propose the rotation number (RN) as a diagnostic tool to identify the existence and trapping time of stickiness trajectories in Hamiltonian systems. Let $\mathbf{x} \mapsto M^n(\mathbf{x})$ be a map of the circle S^1 onto itself. The RN for the trajectory starting at the point \mathbf{x}_0 is defined as

$$\omega(\mathbf{x}_0) = \lim_{n \rightarrow \infty} \frac{1}{n} \Pi \cdot (M^n(\mathbf{x}_0) - \mathbf{x}_0), \quad (2)$$

where Π is a suitable angular projection. The finite-time rotation number may lead to false interpretation about the stickiness regions. For short simulation times, the stickiness region can be identified as an island. However, the RN is able to identify the island, chaotic sea, and stickiness.

We assume that the RN exists for a given position in the phase space, then we monitor $|\nabla\omega|$ during a long time interval ($N = 10^7$). In the islands, there is no divergence of the RN when time tends to infinity ($n \rightarrow N$). For the chaotic trajectories, the RN is not defined, and as a consequence, the gradient of the RN does not converge. Even so, $|\nabla\omega|$ diverges much faster in the chaotic orbit initiated outside than that inside the sticky domain due to the trapping time.

When the trajectories leave the sticky region and enter into the chaotic sea, there is an abrupt change in the $|\nabla\omega|$. The time interval that this change takes to occur is the trapping time. Figure 4 shows examples of the trapping time obtained with this procedure. The advantage is that we do not need to know the position of the islands in the phase space. Figure 4 displays magnifications of the trapping times in the phase space for $K = 6.908745$. The trapping times reveal the presence of the microstructures around the islands. The result is similar in appearance to Fig. 3, but without determining the positions (box) of the islands in the phase space.

In Fig. 5, we compute the statistics trapping times through the RN, where the stickiness domains are divided into three intervals according to the magnifications shown in Fig. 4. Interval A corresponds to the chaotic sea and intervals B, C, and D represent different layers of stickiness. The long trapping times are connected to small areas of the stickiness domains in the phase space. We verify, for one chaotic orbit, that the trapping time distribution as a function of τ follows a power law for each stickiness region.

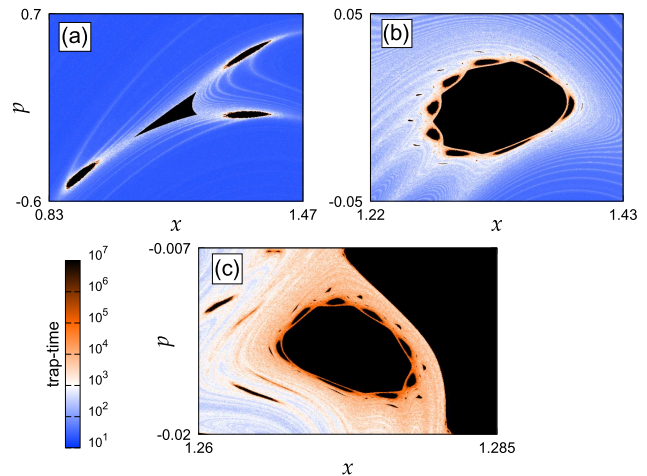


FIG. 4. Trapping time calculated through RN for the SM. The figures display magnifications around the island for $K = 6.908745$.

Figure 6 exhibits the stickiness/grid (STK/G) for the values of K , where the sticky orbits exist. For $STK/G > 0$, we identify the appearance of sticky domains. We divide the phase space into a grid of 800×800 points to create a wide set of initial conditions for $N = 10^4$ in the first layer (region B in Fig. 5) of the stickiness region. We see that the size of the stickiness region depends on the K value. With regard to the nonlinearity parameter K , Meiss *et al.*²⁶ studied diffusion coefficients and correlation functions in area-preserving maps and reported that the decay law for the correlations depends sensitively on K . They verified that the agreement between the theory and numerical experiments is poor in the presence of islands in the phase space, even if the trajectories never enter into the island region.

In Fig. 7, we compare the trapping time distributions for different values of K . For K equal to 7.072394 (red balls), the SM has no stickiness domains, and as a consequence, the τ values are less than 10^2 . When K is equal to 6.567797 (blue balls) and 6.855315 (black balls), the SM presents large and intermediate sticky regions,

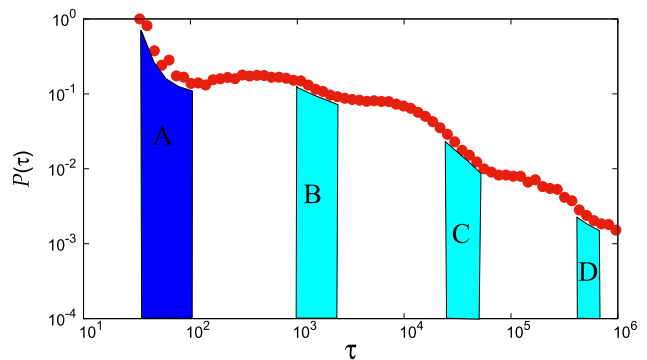


FIG. 5. Divergence time distribution $P(\tau)$ for $K = 6.908745$. A corresponds to the chaotic sea and intervals B, C, and D represent different layers of stickiness.

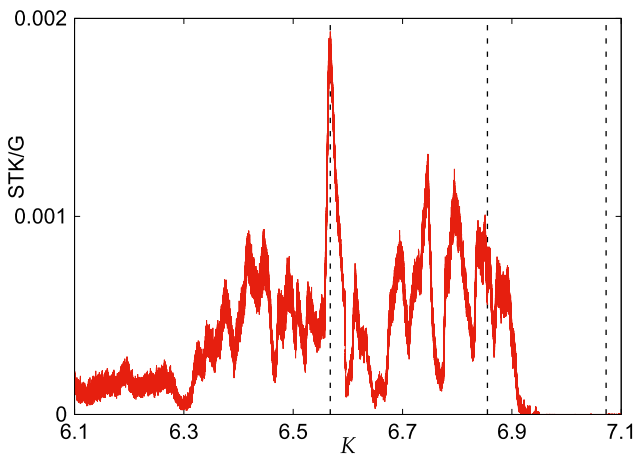


FIG. 6. Stickiness/grid (STK/G) vs K . We consider $N = 10^4$ and a grid of 800×800 initial conditions in all phase space.

respectively. The existence of stickiness domains is characterized by different decay coefficients in the distribution. These different coefficients are due to chaotic and quasiregular motions.⁹

Szezech *et al.*¹⁶ showed that the distribution of finite-time Lyapunov exponents (FTLE) can be used to detect trap effects in Hamiltonian systems. The j th time- n Lyapunov exponent associated with the point (p_0, x_0) is defined as

$$\lambda_j(p_0, x_0, n) = \frac{1}{n} \ln \| DM^n(p_0, x_0) W_j \| \quad (j = 1, 2), \quad (3)$$

where DM^n and W_j are the Jacobian matrix and the eigenvector, respectively.¹⁶ Figure 8(a) shows the FTLE (black line) and the RN (red line) as a function of K . The FTLE is calculated by means of $N = 10^9$ iterations, while for the RN, we consider $N = 10^4$ and a phase space grid of 800×800 . Therefore, fewer iterations are required and there is no need for computation of the Jacobian matrix to compute RN than FTLE to identify the stickiness phenomenon. In Figs. 8(b)

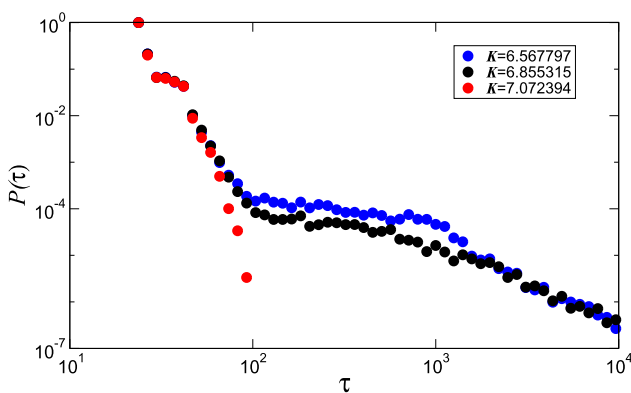


FIG. 7. Trapping time distributions for K equal to 6.567797 (blue balls), 6.855315 (black balls), and 7.072394 (red balls).

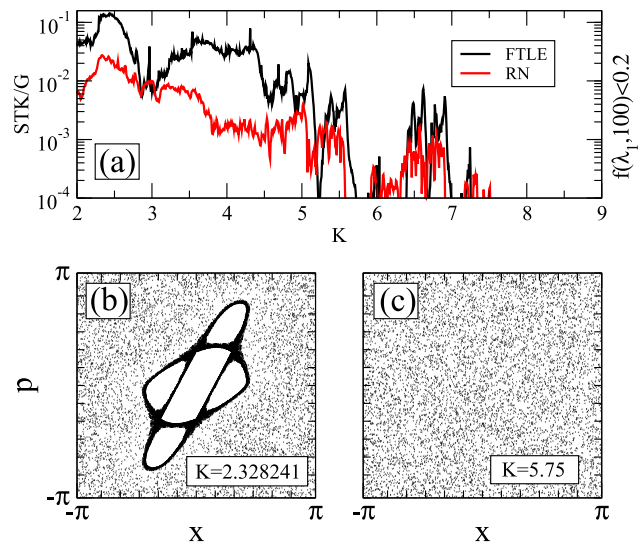


FIG. 8. (a) Function distribution FTLE, $f(\lambda_1, 100) < 0.2$ (black line), and STK/G (RN) (red line) as a function of K . (b) and (c) show the phase space for $K = 2.328241$ and $K = 5.75$, respectively.

and 8(c), we see the phase space with sticky regions and chaotic orbits, respectively.

IV. CONCLUSIONS

We study the stickiness of chaotic orbits. The stickiness is an effect that is difficult to identify in the Hamiltonian systems. In this work, we propose the use of the rotation number as a new diagnostic tool to detect stickiness. Here, its small nondivergence is used as an indication of stickiness. We apply the proposal procedure to the standard map.

Our results show that the gradient of the rotation number (RN) detects, much faster than other proposed procedures, the existence of sticky domains in the phase space. Our procedure is proper to be used for different values of the nonlinear control parameters. With this faster indicator, it is possible to find the stickiness regions in the phase space and to calculate the trapping times.

We calculate the stickiness/grid (STK/G) using the RN and verify that the results are similar to the finite-time Lyapunov exponents (FTLE). One advantage is that the simulations of the STK/G need fewer iterations than the FTLE, as well as it is not necessary to calculate the Jacobian matrix. The simultaneous presence of positive high and low values of FTLE in time series is a fingerprint of stickiness; however, for this to be true, the initial conditions must be within the chaotic sea, i.e., outside an island; therefore, it is necessary to know the positions of the islands in the phase space. Then, other import outcome is related to the lack of knowledge the island positions to compute the RN. Therefore, by means of the RN, there is no need of information about the islands to detect the existence of stickiness and to calculate the trapping times.

ACKNOWLEDGMENTS

This work was made possible by the support from the following Brazilian government agencies: CNPq (No. 150701/2018-7), FAPESP, CAPES, and Fundação Araucária.

REFERENCES

- ¹S. Aubry, *Physica D* **7**, 240 (1983).
- ²E. L. Lameu, C. A. S. Batista, A. M. Batista, K. Iarosz, R. L. Viana, S. R. Lopes, and J. Kurths, *Chaos* **22**, 043149 (2012).
- ³A. P. Kuznetsov, A. V. Savin, and D. V. Savin, *Physica A* **387**, 1464 (2008).
- ⁴R. R. Stein and H. Isambert, *Phys. Rev. E* **84**, 051904 (2011).
- ⁵I. L. Caldas, R. L. Viana, C. V. Abud, J. C. D. Fonseca, Z. O. Guimarães Filho, T. Kroetz, F. A. Marcus, A. B. Schelin, J. D. Szezech, Jr., D. L. Toufen, S. Benkadda, S. R. Lopes, P. J. Morrison, M. Roberto, K. Gentle, Y. Kuznetsov, and I. C. Nascimento, *Plasma Phys. Control Fusion* **54**, 124035 (2012).
- ⁶B. V. Chirikov, *Phys. Rep.* **52**, 263 (1979).
- ⁷T. Y. Petrosky, *Phys. Lett. A* **117**, 328 (1986).
- ⁸J. D. Meiss, *Rev. Mod. Phys.* **64**, 795 (1992).
- ⁹R. Dvorak, G. Contopoulos, C. Efthymiopoulos, and N. Voglis, *Planet Space Sci.* **46**, 1567 (1997).
- ¹⁰G. Contopoulos, *Nonperiodic Orbits Astron. J.* **76**, 147 (1971).
- ¹¹C. F. F. Karney, *Physica D* **8**, 360 (1983).
- ¹²C. Efthymiopoulos, G. Contopoulos, N. Voglis, and R. Dvorak, *J. Phys. A* **30**, 8167 (1997).
- ¹³G. Contopoulos and M. Harsoula, *Int. J. Bifurcat. Chaos* **18**, 2929 (2008).
- ¹⁴Y. Zou, M. Thiel, M. C. Romano, and J. Kurths, *Chaos* **17**, 043101 (2007).
- ¹⁵C. V. Abud and R. E. Carvalho, *Phys. Rev. E* **88**, 042922 (2013).
- ¹⁶J. D. Szezech, Jr., S. R. Lopes, and R. L. Viana, *Phys. Lett. A* **335**, 394 (2005).
- ¹⁷J. D. Szezech, Jr., A. B. Schelin, I. L. Caldas, S. R. Lopes, P. J. Morrison, and R. L. Viana, *Phys. Lett. A* **377**, 452 (2013).
- ¹⁸J. D. Szezech, Jr., I. L. Caldas, S. R. Lopes, P. J. Morrison, and R. L. Viana, *Phys. Rev. E* **86**, 036206 (2012).
- ¹⁹K. M. Frahm and D. L. Shepelyansky, *Eur. Phys. J. B* **76**, 57 (2010).
- ²⁰J. D. Howard and S. M. Hohns, *Phys. Rev. A* **29**, 418 (1984).
- ²¹S. Benkadda, S. Kassibrakis, R. B. White, and G. M. Zaslavsky, *Phys. Rev. E* **55**, 4909 (1997).
- ²²F. M. Izraelev, *Physica D* **1**, 243 (1980).
- ²³S. R. Lopes, J. D. Szezech, Jr., R. F. Pereira, A. A. Bertolazzo, and R. L. Viana, *Phys. Rev. E* **86**, 016216 (2012).
- ²⁴T. S. Krüger, P. P. Galuzio, T. L. Prado, R. L. Viana, J. D. Szezech, Jr., and S. R. Lopes, *Phys. Rev. E* **91**, 062903 (2015).
- ²⁵G. M. Zaslavsky, *Physica D* **168**, 292 (2002).
- ²⁶J. D. Meiss, J. R. Cary, C. Grebogi, J. D. Crawford, A. N. Kaufman, and H. D. I. Abarbanel, *Physica D* **6**, 375 (1983).